Palladium Nanoparticles on Modified Cellulose as a Novel Catalyst for Low Temperature Gas Reactions

Esteban Gioria
INCAPE: Instituto de Investigaciones en Catalisis y Petroquimica
Chiara Signorini
INCAPE: Instituto de Investigaciones en Catalisis y Petroquimica
María Claudia Taleb
Universidad Nacional del Litoral Facultad de Ingenieria Quimica
Magdolna Mihályi
Research Centre for Natural Sciences Institute of Materials and Environmental Chemistry: Termeszettudomanyi Kutatokozpont Anyag- es Kornyezetkemiai Intezet
Laura Gutierrez (lbgutier@fiq.unl.edu.ar)
INCAPE: Instituto de Investigaciones en Catalisis y Petroquimica

Original Research

Keywords: palladium, cellulose, environmental catalysis, H2-SCR, selective catalytic reduction.

Posted Date: May 13th, 2021

DOI: https://doi.org/10.21203/rs.3.rs-192931/v1

Version of Record: A version of this preprint was published at Cellulose on August 7th, 2021. See the published version at https://doi.org/10.1007/s10570-021-04118-9.

Abstract

Palladium was incorporated into carboxymethylated cellulose fibers as a support, thereby becoming an efficient and stable catalyst for low temperature gas phase reaction. Thus, NO was used as test molecule of Greenhouse Gas to be catalytically reduced with hydrogen on an eco-friendly sustainable material containing palladium as the active site. Prior to the catalytic test, the catalysts were reduced with glucose as an eco-friendly reagent. The material characterization was performed by SEM-EDS, XRD, LRS, TGA and FTIR.

The catalytic results showed that at 170°C, NO conversion was 100% with a selectivity of 70% to nitrogen. While NO_X species were completely converted into N_2 at temperatures higher than 180°C. The starting commercial material Solucell® was also studied, but its performance resulted lower than the ones of functionalized fibers.

The use of this strategy, i.e., the functionalization of cellulose fibers followed by in-situ formation of metallic nanoparticles, can be further applied for the design of a wide range of materials with interesting applications for gas and liquid phase reactions under mild conditions.

1. Introduction

The degradation of the equilibrium of the environment caused by human activity and the consumption of natural resources for energy production and general inputs is a matter of global concern and growing importance (Letcher 2019; Qiao et al. 2019). The increment of the greenhouse gases (GHGs) concentration in the atmosphere straightly affects climatic parameters (planet global temperature, changes in rainfall patterns, extreme weather events, among others) (Arnell 1999; Jacob and Winner 2009; Kumar et al. 2018). Consequently, researchers and the scientific community stay alert looking for new and optimal strategies to control emissions from different productive activities. Nitrogen oxides (NO_X) emissions from the motor vehicle exhausts, and the combustion of coal, oil or natural gas, are among the main GHGs (Lammel and Graßl 1995; Hamada and Haneda 2012; Boningari and Smirniotis 2016).

The well-known NO_x catalytic treatment of mobile or stationary sources involves the use of technologies and procedures that often lead to high-energy consumption and high equipment costs (Piumetti et al. 2015; Serrano et al. 2019). The optimization of these methodologies is sometimes associated with the modification of reactor devices; the synthesis of catalytic materials in which the cost of reagents is high as well as with the generation of harmful by-products or wastes during the production stages (Praveena and Martin 2018).

In this context, the reduction of NO_X employing hydrogen as reducing agent (H_2-SCR) has recently been proposed as an effective and eco-friendly technology for the treatment of this gas and several active catalytic systems were reported (Fu et al. 2014; Wang et al. 2016; Resitoglu and Keskin 2017; Gioria et al.

2019a). Hence, we propose the synthesis of a novel catalytic material for the selective reduction of NO_X to nitrogen, based on modified cellulose with metallic palladium nanoparticles as active sites.

Cellulose is the most abundant natural polymer, and it is present in most of the terrestrial biomass. Through several functionalization processes, it is possible to incorporate different functional groups into their polymeric chains. This allows changing the original material composition and structure, adapting it as a support for a wide variety of adsorbent and catalyst applications. Consequently, these physicochemical surface modifications of the cellulose also could give rise to the possibility of anchoring metallic entities on the structure. Therefore, the novelty of this work is that palladium is incorporated into the modified cellulose as an active phase, thereby becoming an efficient catalyst for the gas phase reaction.

Palladium was selected as the active metal owing to its high hydrogen spillover ability and its high activity for the H_2 and NO activation in the H_2-SCR (YU et al. 2010; Patel and Sharma 2020). In addition, palladium is employed for numerous low temperature catalytic reactions, required to preserve the stability of the cellulosic fibers. In order to optimize the anchoring process of the metallic nanoparticles, a study of the cellulose derivatization with carboxymethyl group using different solvents was proposed (Dong and Hinestroza 2009; Song et al. 2012; Nishikata et al. 2014).

In this work, an effective catalyst for the mentioned reaction is presented, using modified cellulose as a novel support since it is an inexpensive and abundant biodegradable natural material.

Within the recent years, several researchers have reported the use of cellulose supporting palladium as active site. Mainly, hydrogenation and cross-coupling reactions in liquid phase were studied (Nishikata et al. 2014; Zheng et al. 2015; Li et al. 2017b, 2018; Gopiraman et al. 2018; Lu et al. 2018; Xiang et al. 2018; Islam et al. 2019; Seyednejhad et al. 2019; Dong et al. 2019; Kempasiddaiah et al. 2020; Yamada et al. 2020). However, and to the best of our knowledge, this is the first report where cellulose is employed as an effective catalytic support for the gas-phase reduction of NO, reaction of environmental concern.

2. Experimental

2.1. Catalyst Synthesis

Synthesis of carboxymethylated cellulose fibers (CMF)

Eucalyptus-dissolving pulp (Solucell®, α-cellulose) provided by Bahia Specialty Cellulose S.A., Camacari, Brazil, was employed as raw material.

It is well known that the cellulose functionalization with sodium monochloroacetate involves the replacement of the -OH groups in the anhydrous glucose units (AGU) by carboxyl groups. In heterogeneous conditions, this reaction takes place in two stages: mercerization and etherification (Togrul 2003).

The mercerization was carried out in a round flask under reflux at 25 ºC during 90 min with magnetic stirring. The reaction mixture consisted of 3 g of cellulose fibers, 150 ml of a specific solvent (ethanol, isopropanol or deionized water) and 30 ml of a 30% w/w solution of sodium hydroxide (99% Cicarelli).

After that, and for the etherification step, 4.5 g of sodium monochloroacetate (99 % Sigma-Aldrich) dissolved in 10 ml of distilled water were added, keeping the temperature at 30ºC during 1 h. Before filtration, the final suspension was neutralized (pH = 6-8) with 90% (v/v) acetic acid (Cicarelli).

The carboxymethylated cellulose (CMF) was washed several times with 80% ethanol, filtered and stored at 5-8ºC until further use. The degree of substitution (DS), defined as the number of the carboxymethyl groups in the molecular unit of the anhydroglucose units, was determined by the standard method (ASTM D1439-03). The carboxyl content of pulp was measured according to the TAPPI T 237 cm-98 norm. While, the water solubility of carboxymethylated pulp was evaluated by the residual solid quantification (Shui et al. 2017). The supports were named CMFE, CMFIP and CMFW according to the solvent used in the mercerization stage, CMF: carboxymethylated cellulose fibers; E, IP and W: ethanol, isopropanol and water respectively. In order to analyze the degree of substitution, the samples were compared to commercial carboxymethylcellulose (CMC, Sigma Aldrich 99 %).

Incorporation of Pd on the cellulosic supports

In order to prepare the palladium-based catalyst, 100 mg of CMF fibers of carboxymethylated cellulose were sonicated during 30 min in 5 ml of 53 mM $PdCl_2$ solution (Vega & Camji). The pH was fixed to 7 with NaOH (Merck). After that, the suspension was heated in a water bath at 80°C during 1h, filtered and washed with deionized water. The final Pd impregnated fibers (CMFE.Pd) were dried overnight at 80°C.

For the sake of comparison, palladium was also added onto the starting non-modified Solucell® following the same protocol. The final material was named Solucell.Pd.

Following the principles of “Green chemistry”, the use of hazardous and toxic reagents was avoided. Consequently, glucose was employed as a mild reducing agent. The reduction of the materials containing Pd (CMFE.Pd and Solucell.Pd) was carried out with an 8.3 mM glucose solution for 10 min at 60°C (Gioria et al. 2019b). After this step, the suspensions were filtered, washed several times with deionized water and dried overnight at 80°C. The final catalysts were named CMFE.Pd.Gluc and Solucell.Pd.Gluc.

2.2 Material characterization

The identification of the different crystalline species was done by X-ray diffraction analysis (DRX, Shimadzu XD-D1). In addition, temperature programmed XRD studies under reducing atmosphere were carried out. Using a H_2 flow of 50 $ml.min^{-1}$ and a heating rate of 5 $°C.min^{-1}$, XRD diffractograms were recorded at room temperature (before and after heating) and at 200°C.

Fourier Transform Infrared Spectroscopy (FTIR, Thermo-Mattson model Genesis II) and Laser Raman Spectroscopy (LSR, Horiba Labram HR) determined the nature of the functional groups. The macroscopic

aspect at each stage of the synthesis was observed with an Olympus SZ51 optical stereo microscope.

The surface morphology of the material was studied using scanning electron microscopy (SEM benchtop Phenom ProX) and the chemical composition was analyzed by X-ray energy dispersion spectrometry (EDX), in mapping mode. In addition, Field emission scanning electron microscopy (FE-SEM) was employed at higher magnification in a ZEISS GeminiSEM500 NanoVP.

The thermogravimetric analysis (TGA-SDTA) was performed in a Mettler Toledo STAR analyzer with a TGA/SDTA851e module. A 70 µL alumina crucible containing 30-40 mg of sample was heated from 30 °C to 800 °C in air flow (50 ml.min^{-1}). The heating rate was fixed at 10 °C.min^{-1}.

2.3 Catalytic evaluation

The reduction of NO with H_2 was carried out in a quartz fixed bed reactor operating at atmospheric pressure, placed in a temperature-controlled furnace. The GHSV was fixed at 2500 h^{-1}, with a feed composition of 1000 ppm of NO and 2% H_2 using He for balancing and regulated by mass flow controllers. The temperature range evaluated was 30 up to 200°C with a heating rate of 10 °C.min^{-1}, in order to preserve the thermal stability of the fibers in agreement with the previous TGA analysis.

The concentrations of the reactor effluent gases (NO, NO_2, N_2O and NH_3) were monitored every 2 minutes with an on line FTIR Mattson Genesis II (resolution of 4 cm^{-1}) instrument equipped with a 15 cm path length gas IR cell with CaF_2 windows at room temperature. The N_2 production was calculated by atomic nitrogen balance. The NO conversion (C_{NO}) and the selectivity to N_2 (S_{N2}) were calculated as follows:

$$C_{NO} = ([NO]^0 - [NO]) / [NO]^0 \qquad \text{(Eq. I)}$$

$$S_{N2} = ([NO]^0 - [NO] - [NO_2] - 2[N_2O] / [NO]^0 \qquad \text{(Eq. II)}$$

where $[NO]^0$ is the initial concentration of NO, whereas [NO], $[NO_2]$ and $[N_2O]$ are the concentrations of the corresponding components in the reactor effluent.

3. Results

The cellulose functionalization with sodium monochloroacetate involves the partial replacement of the polymeric matrix -OH terminals by carboxyl groups. The substitution degree (DS) is a crucial factor that defines the water solubility of the carboxymethylated cellulose. It is established that the polymer is insoluble but swellable when DS values are below ca. 0.4 (Togrul 2003). On the other hand, in the carboxymethylation reaction, the role of the solvent is to provide the etherifying reagent accessibility into the reaction centres of the cellulosic chain. Consequently, the solvent polarity index (P) is an important property, as it affects the efficiency of this reaction: the bigger the polarity, the lower DS (P_{water}=1, $P_{ethanol}$= 0.655, P_{isop}= 0.546) (Pushpamalar et al. 2006). The water solubility, degree of substitution (DS)

and carboxyl group content (CG) obtained for the prepared fibers are given in Table 1. The degree of substitution (DS), defined as the number of the carboxymethyl groups in the molecular unit of the anhydroglucose units, was determined by the standard method (ASTM D1439-03). The carboxyl content of pulp was measured according to the TAPPI T 237 cm-98 norm. While, the water solubility of carboxymethylated pulp was evaluated by the residual solid quantification.

Table 1. Properties of the prepared carboxymethylated fibers.

Sample	S_{water} (%)	DS	CG (meq/100g)
Solucell	Insoluble	n.a	0.7
CMFW	4.7	0.18	37.8
CMFE	4.6	0.21	38.9
CMFIP	6.9	0.24	40.1

S_{water}: solubility in water, DS: degree of substitution, CG: carboxyl group content.

The three cellulose etherification methods yielded the expected results, i.e. the less polar solvent brought about the best reaction efficiency and the highest water solubility compared to the other solvents (CMFIP).

The normalized FTIR spectra (Figure 1) reveal the different degrees of substitution of the prepared functionalized fibers. The FTIR spectrum of the commercial pure CMC (DS= 0.8) presents two main bands at ca. 1600 and 1420 cm^{-1} in the range 1900-1350 cm^{-1} due to the carboxylate groups symmetric and asymmetric stretching vibrations (Biswal and Singh 2004; Riaz et al. 2018). These bands could be clearly observed in the CMFE and CMFIP. They could also be seen in the CMFW sample but with lower intensity compared with the CMC fiber. This conclusion could be corroborated with the absence of such bands in the spectrum of the non-modified support (Solucell).

It could be observed that when ethanol or isopropanol were used for the functionalization, similar results were obtained. Moreover, comparable degree of substitution and carboxyl group content were determined. In order to apply environmentally friendly protocols that follow the principles of “Green Chemistry”, and taking into account that ethanol is cheaper and less toxic than isopropanol (Beach et al. 2009), the carboxymethylated fibers with ethanol were chosen for the anchoring of palladium nanoparticles. For the sake of comparison, the starting material (Solucell®) was also impregnated with palladium. Thereby, Figure S.1 shows the macroscopic aspect of the Solucell, CMFE and the impregnated Solucell.Pd and CMFE.Pd fibers.

The Scanning electron microscopy (SEM) micrographs are shown in Figure 2. The presence of palladium on the matrix was detected by X-Ray spectroscopy (EDX) (Figure 3). The chemical analysis evidenced 11% of Pd loading on the CMFE.Pd sample and 6% in the Solucell.Pd fibers. In order to verify these

results, the palladium content was also analyzed by thermal gravimetric analysis; resulting 9.5% and 7.3% for CMFE.Pd and Solucell.Pd respectively (as it shows in Figure 7).

The Raman spectra of CMFE.Pd and Solucell.Pd samples together with the CMFE support, are displayed in Figure 4. Pd-Cl complex species, indicating the presence of partially oxidized palladium species could be observed in the palladium containing material. The signals in 251 cm^{-1} correspond to species of type Cl-Pd-Cl, while the signal at 650 cm^{-1} is characteristic of PdO (Baylet et al. 2011). On the other hand, the signals at 439, 581 and 648 cm^{-1} are characteristics of $PdO_{X/2}Cl_{2-X}$ species. In addition, the bands at 330-380 and 893 cm^{-1} correspond to the cellulosic support (Agarwal 2019).

In addition, temperature programmed XRD studies under reducing atmosphere were carried out. Using a H_2 flow of 50 $ml.min^{-1}$ and a heating rate of 5 $°C.min^{-1}$, XRD diffractograms were recorded at room temperature (before and after heating) and at 200°C. For the CMFE.Pd.Gluc sample (after reduction in glucose solution), PdH_x phase can be detected at room temperature, before heating and after cooling down (Figure 5.B). At 200°C, metallic fcc palladium is formed (JCPDS 03-065-6174). The mean crystallite size was determined using the Scherrer's equation, indicating small crystallites of 20 nm.

After reducing treatment with glucose, the fibers were analyzed by Field emission scanning electron microscopy. For the non-functionalized fibers, isolated and non-uniform particles were observed (Figure 6.a-c). However, well-dispersed and uniform palladium nanoparticles were detected on the functionalized CMFE.Pd.Gluc fibers (Figure 6.d-f).

Carboxymethylated cellulose fibers have been reported as an economic and environmentally friendly adsorbent for different metallic ions in solution (Ashraf et al. 2014; Zhu et al. 2016; Ruan et al. 2016; Bediako et al. 2016; Li et al. 2017a; Rossi et al. 2018; Wang et al. 2019). This property can be related to different contributions: the incorporation of a carboxyl functional group and the modification of the crystalline structure of the cellulose. Equation (III) simplifies the interaction between the carboxyl functional group and divalent metallic ions. This interaction is stronger than in the case of hydroxyl groups in the cellulose, therefore the final metal loading is increased.

$$2\ RCOO^-Na^+ + M^{2+} \rightarrow (RCOO^-)_2M^{2+} + 2\ Na^+ \qquad \text{(Eq. III)}$$

In addition, the mercerization step modifies the native cellulose (structure type I) in cellulose type II, with a loss of crystallinity degree. The cellulose treatment with high concentrated NaOH solution conduces to the intra- and inter crystalline swelling, where the cleavage of hydrogen bonds increases the distance between cellulose chains. Therefore, the incorporation of the carboxymethyl groups and the adsorption of metallic ions could be improved (Wang et al. 2017). These effects were confirmed by calculating the crystallinity index employing the following equations:

$$CrI_I = \frac{I_{[200](22.4°)} - I_{am(18°)}}{I_{[200](22.4°)}}$$

$$CrI_{II} = \frac{I_{[020](20.1°)} - I_{am(16°)}}{I_{[020](20.1°)}}$$

Where Cr_{II} and Cr_{III} correspond to the crystallinity index for cellulosic fibers type I and II, respectively (Nam et al. 2016). The intensity data were measured from the XRD analysis show in Figure 5.a. As a result, crystallinity of Solucell and CMFE resulted 74.8% and 13.4%, respectively (Table 2).

Table 2. Crystallinity index of the fibers determined by Segal method

Crystallinity Index (%)	
Solucell	74.8
Solucell.Pd	52.5
Solucell.Pd.Gluc	38.5
CMFE	13.4
CMFE.Pd	10.6
CMFE.Pd.Gluc	8.7

On the other hand, a possible reaction pathway between the cellulose and the metallic ions was proposed by Wu et al. (Wu et al. 2013). The electron-rich hydroxyl groups in the fibers act as a mild reducing agent forming PdNPs. In this step, hydroxyl groups are oxidized to aldehydes entities. Then, the rich-electronic density of these formed groups could act as an anchor centre for the PdNPs stabilization. In previous works, a similar behavior was observed when suspensions of AgNPs and PdNPs were prepared using glucose and starch (Giorello et al. 2018; Gioria et al. 2019b, 2020). Glucose was employed under the same mild reaction conditions reported in this work. For both Ag and Pd nanoparticles, the reducing role of the glucose was corroborated. Meanwhile starch was used as the stabilizer, anchoring the metallic nanoparticles into the polymeric chains.

This analysis could explain the superior metal loading in the carboxymethylated fibers observed by TGA and EDX analysis. The incorporation of the carboxyl groups modifies the crystalline structure, allowing a better access of the palladium ions and their homogeneous distribution. Also, the incorporated carboxyl groups promote the stabilization of the formed PdNPs by electrostatic interactions. The modified structure by the addition of new carboxyl groups could allow a better palladium anion accessibility, which finally results in a homogeneous distribution of PdNPs.

Regarding the thermal behavior of the fibers, TGA and SDTA thermogravimetric analyses were carried out (Figure 7). The modified cellulose-based catalyst showed a thermal stability up to 300 °C, which makes it competitive with traditional inorganic catalysts such as Pd/Al_2O_3, Pd/TiO_2, Pd/Al_2O_3-TiO_2, $Pd/V_2O_5/TiO_2$/SBA-15 and $Pd/V_2O_5/TiO_2$/MCM-41 applied under similar reaction conditions (Caravaggio et al. 2016; Wang et al. 2016; Borchers et al. 2021; Song et al. 2021).

Figure 7.b shows the SDTA analysis. For the fibers containing palladium, it can be clearly observed a sharp and exothermic peak at 317°C. This could be related to the presence of the metallic entities that catalyzes the combustion of the fibers, as it was reported for similar palladium – cellulose based materials (Cai et al. 2009; Ruan et al. 2016; Dong et al. 2019; Shi et al. 2019). However, all fibers are stable up to 300°C. Thus, the reaction conditions assure the stability of the materials.

Figure 8 shows the catalytic performance of both the CMFE.Pd.Gluc and Solucell.Pd.Gluc fibers. In the studied range of temperature, full conversion of NO was observed and only N_2O and N_2 were formed as products. For CMFE.Pd.Gluc, NO is converted with a selectivity of 70% to nitrogen at 160°C. At temperatures higher than 180°C, NO_X species are completely converted into nitrogen. Regarding the catalytic behavior of the Solucell.Pd.Gluc, its performance is lower than for CMFE fibers, with selectivity to N_2 of 52% at 160°C, and 89% at 200°C, the highest temperature analyzed.

In both catalyst, there were no evidence of NO_2 formation, which is in accordance with the reductive atmosphere. In addition, there was no evidence of ammonia formation, indicating the active and selective role of Pd towards the reduction of NO with hydrogen. Only N_2 and N_2O were detected as reaction products. As a trend, it is observed that at low temperatures N_2O appears as an intermediate specie. While the temperature increases, the N_2O concentration decreases, and N_2 increases. This would suggest that at lower temperature, NO is partially reduced to form N_2O. When temperature increases, the intermediate entity is reduced to inert N_2. This tendency is clearly evidenced for CMFE fibers. Meanwhile, for the Solucell fibers temperatures higher than 160°C are needed for a selectivity to N_2 higher than 50%.

4. Conclusions

- Cellulose fibers were successfully functionalized with the partial replacement of hydroxyl groups by carboxymethyl groups:

In this process, three different solvents were tested for the cellulose etherification step (isopropanol, water and ethanol). Ethanol was selected as the most convenient solvent due to its inherent features: it is non-toxic, inexpensive and environmentally friendly.

- Metallic palladium nanoparticles were formed on the surface of the functionalized and no-functionalized fibers by reducing Pd with glucose:

After the impregnation procedure using Pd as precursor, it was possible to increase the metallic loading (7.3% to 9.5%) on the carboxymethylated fibers, and to form well-dispersed palladium metallic nanoparticles using glucose as a green, safe and non-expensive reducing agent.

A battery of techniques such as Raman laser spectroscopy, XRD and TP-XRD under H_2 atmosphere, FTIR and SEM-EDX, conduced to corroborate the presence of palladium species on the polymeric structure and the nature of Pd entities.

- The higher palladium content resulted on the functionalized fibers (CMFE.Pd.Gluc):

This advantage means that the modification of fibers with carboxymethyl groups involves an easier method for the increment of active sites on the cellulosic surface compared with the non-functionalized support.

- The synthetized cellulosic materials with palladium resulted active for the reduction of NO with H_2:

The fibers with the higher palladium content (CMFE.Pd.Gluc) shown enhanced catalytic NO conversion to N_2 in comparison with the raw fibers. The full conversion of NO (X_{NOx}= 100%) to inert nitrogen was completed even at 180 ºC. Even more, the thermal stability up to 300°C assures the competitiveness of the metal-cellulosic fibers, compared with traditional supported catalysts.

In addition, and to the best of our knowledge, the use of cellulose as support for the reduction of NO under mild conditions has never been reported. The use of this strategy can be further conceptualized for the design and development of a wide range of materials with interesting applications for gas and liquid phase reactions under mild conditions.

With this work, a hybrid metal-cellulosic material was synthesized with promising applications on the catalyst and adsorbent fields, such as the reduction of pollutants in water, cross-coupling reactions, and ion adsorption from polluted water, among others. Nevertheless, the challenge of improving the use of cellulose as promising material still guides our research.

Declarations

Conflict of Interest

The authors declare no conflict of interest.

Acknowledgements

The authors are grateful for the financial support provided by the UNL, the National Agency for Scientific and Technological Production (ANPCyT), CONICET and the Ministry of Sc., Techn. and Productive Innovation of Santa Fe (SECTEI). Thanks are also given to Prof. Guillermina Amrein for the English language editing. The authors thank to Dr. José Fernández (Facultad de Ingeniería Química, Universidad

Nacional del Litoral) and Christoph Fahrenson (Zentraleinrichtung Elektronenmikroskopie (ZELMI), Technische Universität Berlin) for performing the SEM-EDS and FESEM observations respectively. The authors also thank for the support in the frame of the bilateral Hungarian-Argentinian science and technology (S&T) cooperation: (i) Hungary: Grant No: TÉT-15-1-2016-0089) and (ii) Argentina: HU-17-01.

Sources of financial support:

Funding acquisition and Project administration by*Laura Gutierrez*

1. National Agency for Scientific and Technological Production (ANPCyT, PICT 2016-2284)-
2. CONICET (PIP- 406)
3. Ministry of Sc., Techn. and Productive Innovation of Santa Fe (SECTEI-2018-2010-038-16).
4. Bilateral Hungarian-Argentinian cooperation project: MINCyT (Argentina)-NKTH (Hungría): HU-17-01

Funding acquisition and Project administration by *Magdolna Miyálgy*

Bilateral Hungarian-Argentinian cooperation project: MINCyT (Argentina)-NKTH: Grant No: TÉT-15-1-2016-0089) in the

Declaration to the ethics committee: The results reported in this manuscript do not involve humans and/or animals researches.

Authors´ Conflicts of Interest: The authors declare no conflict of interest

References

1. Agarwal UP (2019) Analysis of Cellulose and Lignocellulose Materials by Raman Spectroscopy: A Review of the Current Status. Molecules 24:1659. https://doi.org/10.3390/molecules24091659
2. Arnell NW (1999) The effect of climate change on hydrological regimes in Europe: a continental perspective. Glob Environ Chang 9:5–23. https://doi.org/10.1016/S0959-3780(98)00015-6
3. Ashraf S, Saif-ur-Rehman, Sher F, et al (2014) Synthesis of cellulose–metal nanoparticle composites: development and comparison of different protocols. Cellulose 21:395–405. https://doi.org/10.1007/s10570-013-0129-7
4. Baylet A, Marécot P, Duprez D, et al (2011) In situ Raman and in situ XRD analysis of PdO reduction and Pd° oxidation supported on γ-Al2O3 catalyst under different atmospheres. Phys Chem Chem Phys 13:4607. https://doi.org/10.1039/c0cp01331e
5. Beach ES, Cui Z, Anastas PT (2009) Green Chemistry: A design framework for sustainability. Energy Environ Sci 2:1038–1049. https://doi.org/10.1039/b904997p
6. Bediako JK, Wei W, Yun Y-S (2016) Conversion of waste textile cellulose fibers into heavy metal adsorbents. J Ind Eng Chem 43:61–68. https://doi.org/10.1016/j.jiec.2016.07.048

7. Biswal DR, Singh RP (2004) Characterisation of carboxymethyl cellulose and polyacrylamide graft copolymer. Carbohydr Polym 57:379–387. https://doi.org/10.1016/j.carbpol.2004.04.020
8. Boningari T, Smirniotis PG (2016) Impact of nitrogen oxides on the environment and human health: Mn-based materials for the NO x abatement. Curr Opin Chem Eng 13:133–141. https://doi.org/10.1016/j.coche.2016.09.004
9. Borchers M, Keller K, Lott P, Deutschmann O (2021) Selective Catalytic Reduction of NO x with H 2 for Cleaning Exhausts of Hydrogen Engines: Impact of H 2 O, O 2 , and NO/H 2 Ratio. Ind Eng Chem Res acs.iecr.0c05630. https://doi.org/10.1021/acs.iecr.0c05630
10. Cai J, Kimura S, Wada M, Kuga S (2009) Nanoporous Cellulose as Metal Nanoparticles Support. Biomacromolecules 10:87–94. https://doi.org/10.1021/bm800919e
11. Cai Z, Kim J (2010) Bacterial cellulose/poly(ethylene glycol) composite: characterization and first evaluation of biocompatibility. Cellulose 17:83–91. https://doi.org/10.1007/s10570-009-9362-5
12. Caravaggio G, Nossova L, Burich R (2016) Influence of Supports on Pd Catalysts for the Selective Catalytic Reduction of NOx with H2 and CO. Emiss Control Sci Technol 2:10–19. https://doi.org/10.1007/s40825-015-0027-6
13. Dong BH, Hinestroza JP (2009) Metal Nanoparticles on Natural Cellulose Fibers: Electrostatic Assembly and In Situ Synthesis. ACS Appl Mater Interfaces 1:797–803. https://doi.org/10.1021/am800225j
14. Dong Y, Bi J, Zhu D, et al (2019) Functionalized cellulose with multiple binding sites for a palladium complex catalyst: synthesis and catalyst evaluation in Suzuki–Miyaura reactions. Cellulose 26:7355–7370. https://doi.org/10.1007/s10570-019-02568-w
15. Fu M, Li C, Lu P, et al (2014) A review on selective catalytic reduction of NOx by supported catalysts at 100-300°C - Catalysts, mechanism, kinetics. Catal Sci Technol 4:14–25. https://doi.org/10.1039/c3cy00414g
16. Giorello A, Gioria E, Hueso JL, et al (2018) Natural polysaccharides and microfluidics: A win–win combination towards the green and continuous production of long-term stable silver nanoparticles. J Environ Chem Eng 6:5069–5078. https://doi.org/10.1016/j.jece.2018.07.039
17. Gioria E, Marchesini F, Soldati A, et al (2019a) Green Synthesis of a Cu/SiO2 Catalyst for Efficient H2-SCR of NO. Appl Sci 9:4075. https://doi.org/10.3390/app9194075
18. Gioria E, Signorini C, Wisniewski F, Gutierrez L (2020) Green synthesis of time-stable palladium nanoparticles using microfluidic devices. J Environ Chem Eng 8:104096. https://doi.org/10.1016/j.jece.2020.104096
19. Gioria E, Wisniewski F, Gutierrez L (2019b) Microreactors for the continuous and green synthesis of palladium nanoparticles: Enhancement of the catalytic properties. J Environ Chem Eng 7:103136. https://doi.org/10.1016/j.jece.2019.103136
20. Gopiraman M, Deng D, Saravanamoorthy S, et al (2018) Gold, silver and nickel nanoparticle anchored cellulose nanofiber composites as highly active catalysts for the rapid and selective reduction of nitrophenols in water. RSC Adv 8:3014–3023. https://doi.org/10.1039/C7RA10489H

21. Hamada H, Haneda M (2012) A review of selective catalytic reduction of nitrogen oxides with hydrogen and carbon monoxide. Appl. Catal. A Gen. 421–422:1–13
22. Islam MT, Rosales JA, Saenz-Arana R, et al (2019) Rapid synthesis of ultrasmall platinum nanoparticles supported on macroporous cellulose fibers for catalysis. Nanoscale Adv 1:2953–2964. https://doi.org/10.1039/C9NA00124G
23. Jacob DJ, Winner DA (2009) Effect of climate change on air quality. Atmos Environ 43:51–63. https://doi.org/10.1016/j.atmosenv.2008.09.051
24. Kempasiddaiah M, Kandathil V, Dateer RB, et al (2020) Immobilizing biogenically synthesized palladium nanoparticles on cellulose support as a green and sustainable dip catalyst for cross-coupling reaction. Cellulose 27:3335–3357. https://doi.org/10.1007/s10570-020-03001-3
25. Kumar P, Masago Y, Mishra BK, Fukushi K (2018) Evaluating future stress due to combined effect of climate change and rapid urbanization for Pasig-Marikina River, Manila. Groundw Sustain Dev 6:227–234. https://doi.org/10.1016/j.gsd.2018.01.004
26. Lammel G, Graßl H (1995) Greenhouse effect of NOX. Environ Sci Pollut Res 2:40–45. https://doi.org/10.1007/BF02987512
27. Letcher TM (2019) Why do we have global warming? In: Managing Global Warming. Elsevier, pp 3–15
28. Li D, Zhang J, Cai C (2018) Pd Nanoparticles Supported on Cellulose as a Catalyst for Vanillin Conversion in Aqueous Media. J Org Chem 83:7534–7538. https://doi.org/10.1021/acs.joc.8b00246
29. Li G, Li Y, Wang Z, Liu H (2017a) Green synthesis of palladium nanoparticles with carboxymethyl cellulose for degradation of azo-dyes. Mater Chem Phys 187:133–140. https://doi.org/10.1016/j.matchemphys.2016.11.057
30. Li Y, Xu L, Xu B, et al (2017b) Cellulose Sponge Supported Palladium Nanoparticles as Recyclable Cross-Coupling Catalysts. ACS Appl Mater Interfaces 9:17155–17162. https://doi.org/10.1021/acsami.7b03600
31. Lu Z, Jasinski JB, Handa S, Hammond GB (2018) Recyclable cellulose-palladium nanoparticles for clean cross-coupling chemistry. Org Biomol Chem 16:2748–2752. https://doi.org/10.1039/C8OB00527C
32. Nam S, French AD, Condon BD, Concha M (2016) Segal crystallinity index revisited by the simulation of X-ray diffraction patterns of cotton cellulose Iβ and cellulose II. Carbohydr Polym 135:1–9. https://doi.org/10.1016/j.carbpol.2015.08.035
33. Nishikata T, Tsutsumi H, Gao L, et al (2014) Adhesive Catalyst Immobilization of Palladium Nanoparticles on Cotton and Filter Paper: Applications to Reusable Catalysts for Sequential Catalytic Reactions. Adv Synth Catal 356:951–960. https://doi.org/10.1002/adsc.201300691
34. Patel VK, Sharma S (2020) Effect of oxide supports on palladium based catalysts for NO reduction by H2-SCR. Catal Today. https://doi.org/10.1016/j.cattod.2020.04.006
35. Piumetti M, Bensaid S, Fino D, Russo N (2015) Catalysis in Diesel engine NO x aftertreatment: a review . Catal Struct React 1:155–173. https://doi.org/10.1080/2055074x.2015.1105615

36. Praveena V, Martin MLJ (2018) A review on various after treatment techniques to reduce NOx emissions in a CI engine. J Energy Inst 91:704–720. https://doi.org/10.1016/j.joei.2017.05.010
37. Pushpamalar V, Langford SJ, Ahmad M, Lim YY (2006) Optimization of reaction conditions for preparing carboxymethyl cellulose from sago waste. Carbohydr Polym 64:312–318. https://doi.org/10.1016/j.carbpol.2005.12.003
38. Qiao H, Zheng F, Jiang H, Dong K (2019) The greenhouse effect of the agriculture-economic growth-renewable energy nexus: Evidence from G20 countries. Sci Total Environ 671:722–731. https://doi.org/10.1016/j.scitotenv.2019.03.336
39. Resitoglu IA, Keskin A (2017) Hydrogen applications in selective catalytic reduction of NOx emissions from diesel engines. Int J Hydrogen Energy 42:23389–23394. https://doi.org/10.1016/j.ijhydene.2017.02.011
40. Riaz T, Zeeshan R, Zarif F, et al (2018) FTIR analysis of natural and synthetic collagen. Appl Spectrosc Rev 53:703–746. https://doi.org/10.1080/05704928.2018.1426595
41. Rossi E, Montoya Rojo Ú, Cerrutti P, et al (2018) Carboxymethylated bacterial cellulose: An environmentally friendly adsorbent for lead removal from water. J Environ Chem Eng 6:6844–6852. https://doi.org/10.1016/j.jece.2018.10.055
42. Ruan C, Strømme M, Lindh J (2016) A green and simple method for preparation of an efficient palladium adsorbent based on cysteine functionalized 2,3-dialdehyde cellulose. Cellulose 23:2627–2638. https://doi.org/10.1007/s10570-016-0976-0
43. Serrano J, Jiménez-Espadafor FJ, Lora A, et al (2019) Experimental analysis of NOx reduction through water addition and comparison with exhaust gas recycling. Energy 168:737–752. https://doi.org/10.1016/j.energy.2018.11.136
44. Seyednejhad S, Khalilzadeh MA, Zareyee D, et al (2019) Cellulose nanocrystal supported palladium as a novel recyclable catalyst for Ullmann coupling reactions. Cellulose 26:5015–5031. https://doi.org/10.1007/s10570-019-02436-7
45. Shi D, Ouyang Z, Zhao Y, et al (2019) Catalytic Reduction of Hexavalent Chromium Using Iron/Palladium Bimetallic Nanoparticle-Assembled Filter Paper. Nanomaterials 9:1183. https://doi.org/10.3390/nano9081183
46. Shui T, Feng S, Chen G, et al (2017) Synthesis of sodium carboxymethyl cellulose using bleached crude cellulose fractionated from cornstalk. Biomass and Bioenergy 105:51–58. https://doi.org/10.1016/j.biombioe.2017.06.016
47. Song J, Birbach NL, Hinestroza JP (2012) Deposition of silver nanoparticles on cellulosic fibers via stabilization of carboxymethyl groups. Cellulose 19:411–424. https://doi.org/10.1007/s10570-011-9647-3
48. Song J, Wang Z, Cheng X, Wang X (2021) State-of-Art Review of NO Reduction Technologies by CO, CH4 and H2. Processes 9:563. https://doi.org/10.3390/pr9030563
49. Togrul H (2003) Production of carboxymethyl cellulose from sugar beet pulp cellulose and rheological behaviour of carboxymethyl cellulose. Carbohydr Polym 54:73–82.

https://doi.org/10.1016/S0144-8617(03)00147-4

50. Wang J, Dang M, Duan C, et al (2017) Carboxymethylated Cellulose Fibers as Low-Cost and Renewable Adsorbent Materials. Ind Eng Chem Res 56:14940–14948. https://doi.org/10.1021/acs.iecr.7b03697
51. Wang J, Liu M, Duan C, et al (2019) Preparation and characterization of cellulose-based adsorbent and its application in heavy metal ions removal. Carbohydr Polym 206:837–843. https://doi.org/10.1016/j.carbpol.2018.11.059
52. Wang L, Yin C, Yang RT (2016) Selective catalytic reduction of nitric oxide with hydrogen on supported Pd: Enhancement by hydrogen spillover. Appl Catal A Gen 514:35–42. https://doi.org/10.1016/j.apcata.2016.01.013
53. Wu X, Lu C, Zhang W, et al (2013) A novel reagentless approach for synthesizing cellulose nanocrystal-supported palladium nanoparticles with enhanced catalytic performance. J Mater Chem A 1:8645. https://doi.org/10.1039/c3ta11236e
54. Xiang Z, Chen Y, Liu Q, Lu F (2018) A highly recyclable dip-catalyst produced from palladium nanoparticle-embedded bacterial cellulose and plant fibers. Green Chem 20:1085–1094. https://doi.org/10.1039/C7GC02835K
55. Yamada T, Teranishi W, Park K, et al (2020) Development of Carbon-Neutral Cellulose-Supported Heterogeneous Palladium Catalysts for Chemoselective Hydrogenation. ChemCatChem 12:4052–4058. https://doi.org/10.1002/cctc.202000805
56. Yeasmin MS, Mondal MIH (2015) Synthesis of highly substituted carboxymethyl cellulose depending on cellulose particle size. Int J Biol Macromol 80:725–731. https://doi.org/10.1016/j.ijbiomac.2015.07.040
57. YU Q, KONG F, LI L, et al (2010) Fast Catalytic Reduction of NOx by H2 over Pd-Based Catalysts. Chinese J Catal 31:261–263. https://doi.org/10.1016/S1872-2067(09)60045-0
58. Zheng G, Kaefer K, Mourdikoudis S, et al (2015) Palladium Nanoparticle-Loaded Cellulose Paper: A Highly Efficient, Robust, and Recyclable Self-Assembled Composite Catalytic System. J Phys Chem Lett 6:230–238. https://doi.org/10.1021/jz5024948
59. Zhu Y, Wang W, Zheng Y, et al (2016) Rapid enrichment of rare-earth metals by carboxymethyl cellulose-based open-cellular hydrogel adsorbent from HIPEs template. Carbohydr Polym 140:51–58. https://doi.org/10.1016/j.carbpol.2015.12.003

Figures

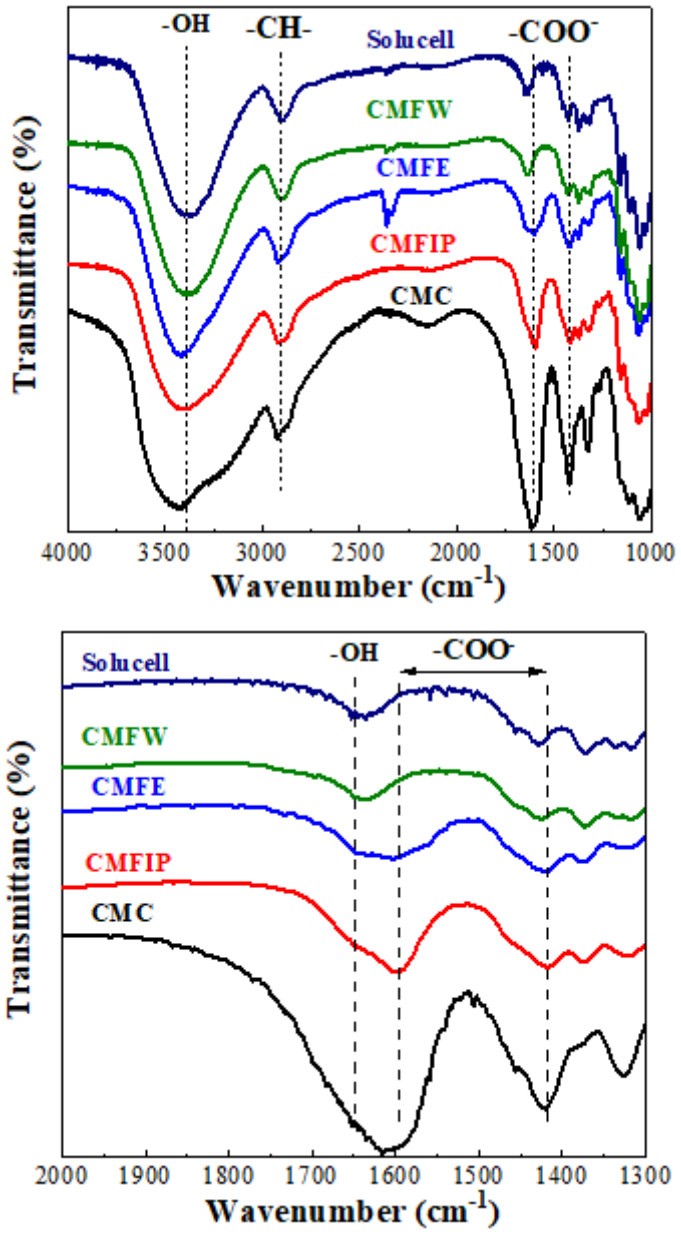

Figure 1

FTIR spectra of the synthetized fibers.

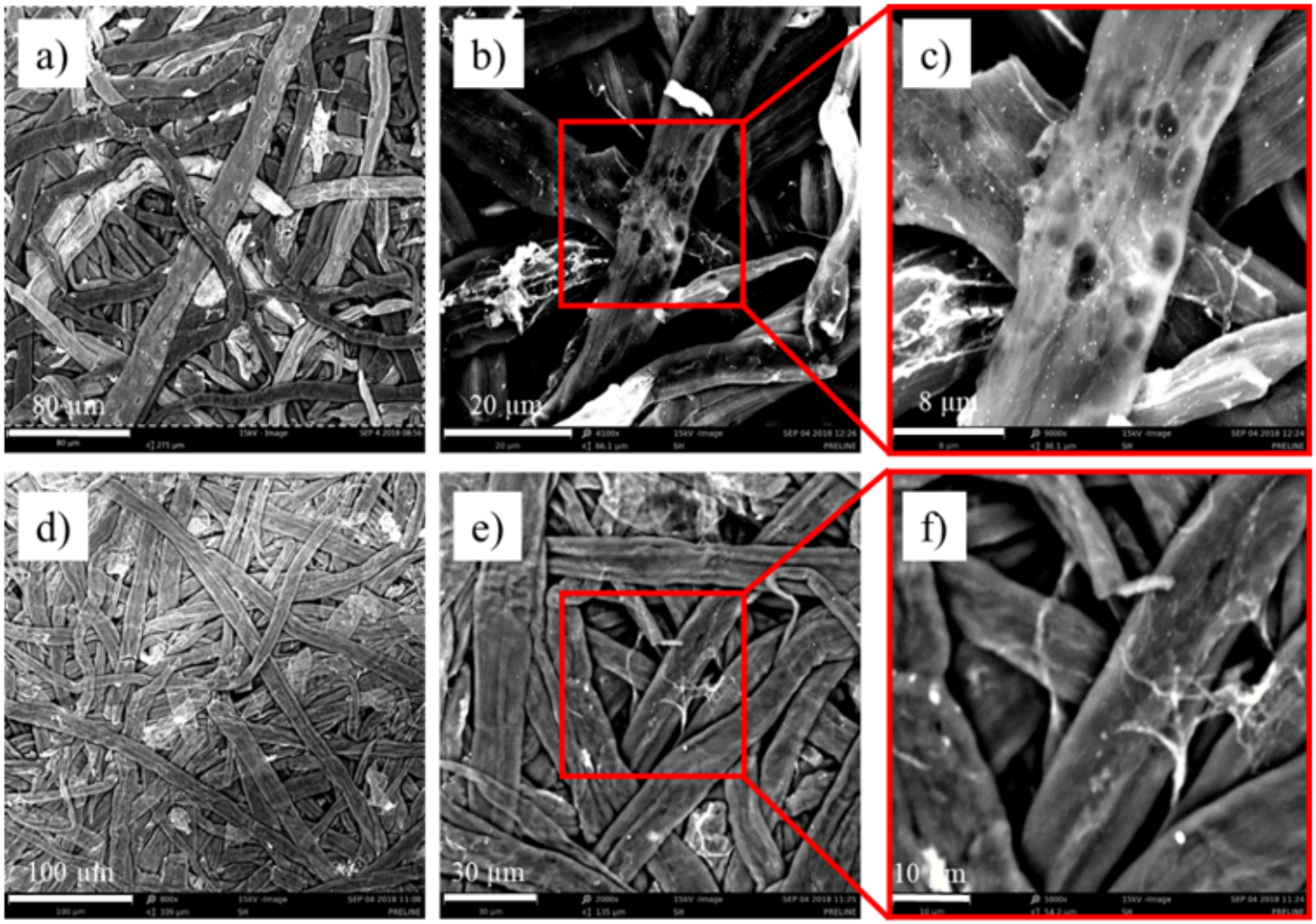

Figure 2

Scanning electron microscopy study of CMFE.Pd (a-c) and Solucell.Pd (d-f)

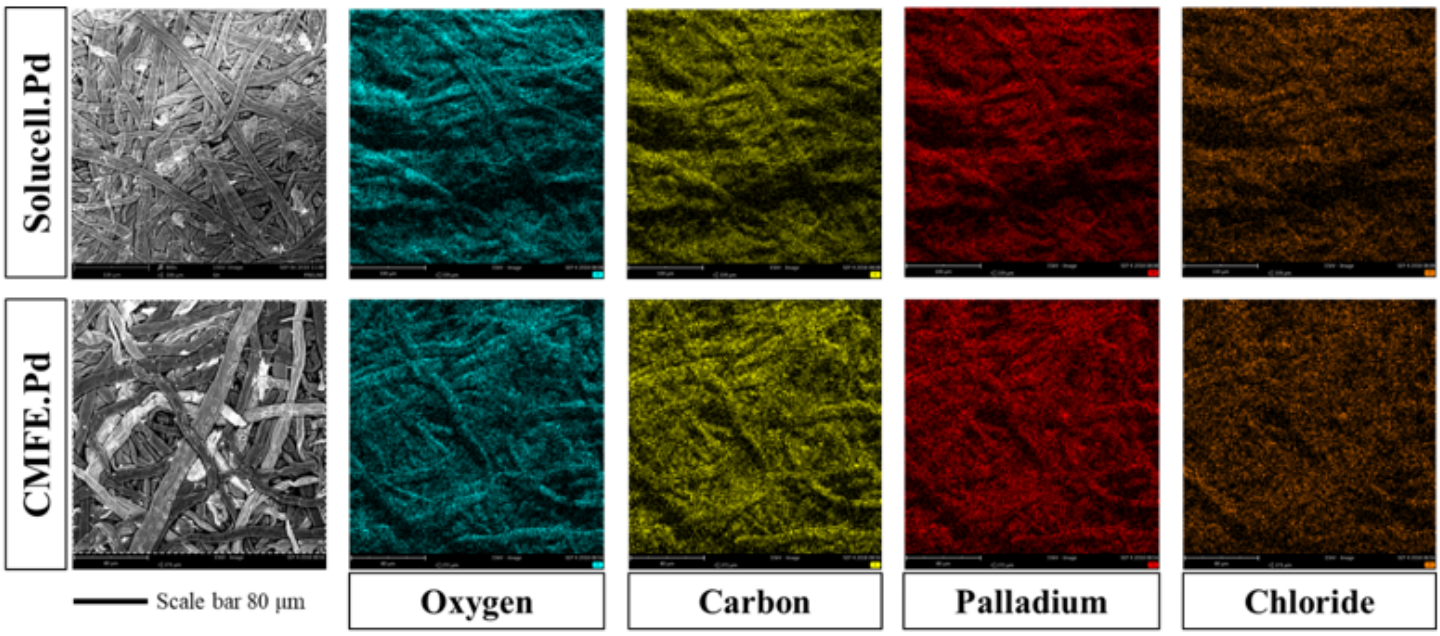

Figure 3

EDX mapping of impregnated Solucell and CMFE fibers.

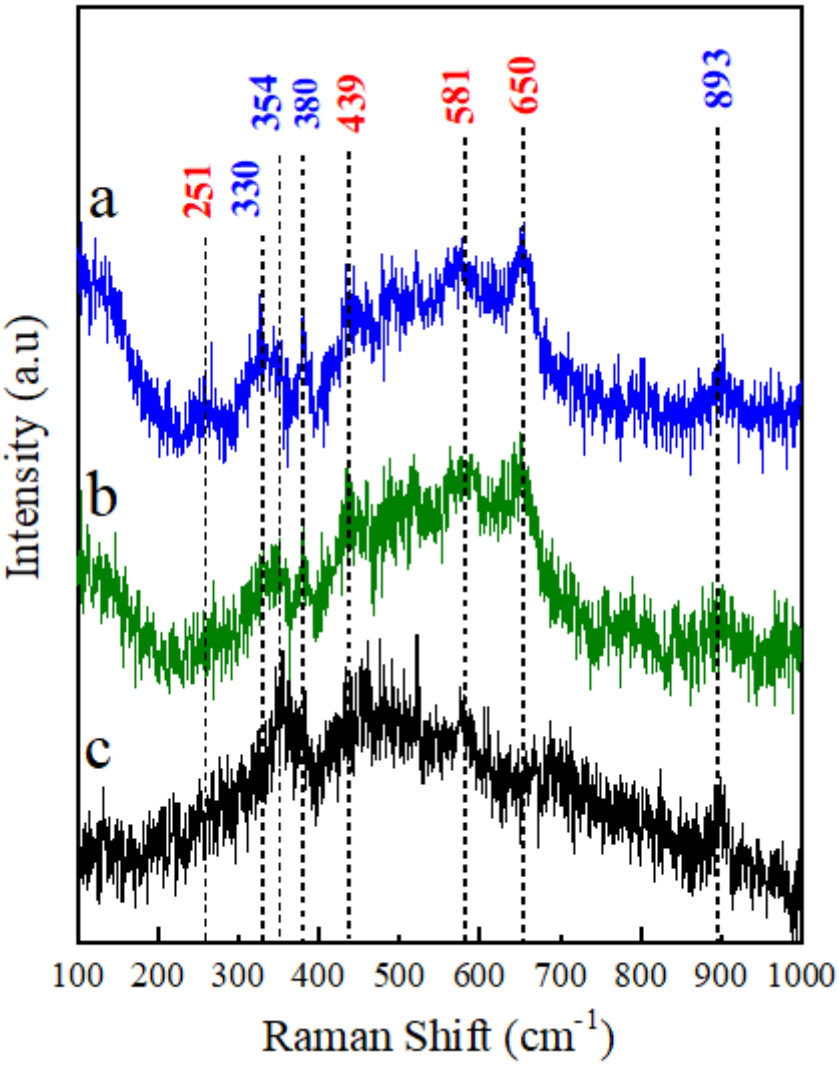

Figure 4

Laser Raman spectra of the synthetized fibers: a) CMFE.Pd; b) Solucell.Pd and c) CMFE fibers.

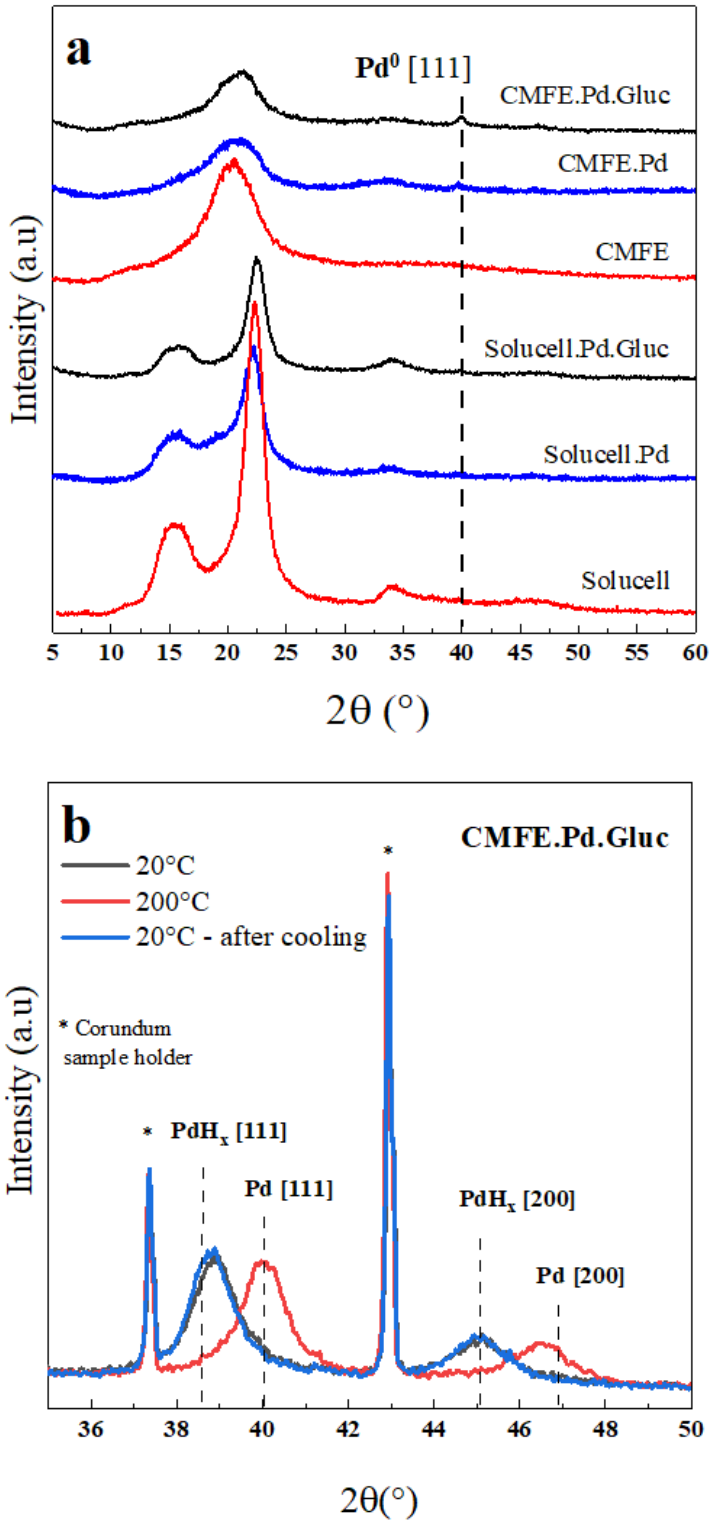

Figure 5

a) XRD patterns of Pd - impregnated samples before and after the reduction with glucose. Cellulosic support is included for comparison. b) TP-XRD patterns under H2 flow of CMFE.Pd.Gluc sample. — room temperature, — 200°C flowing H2 and — after cooling down.

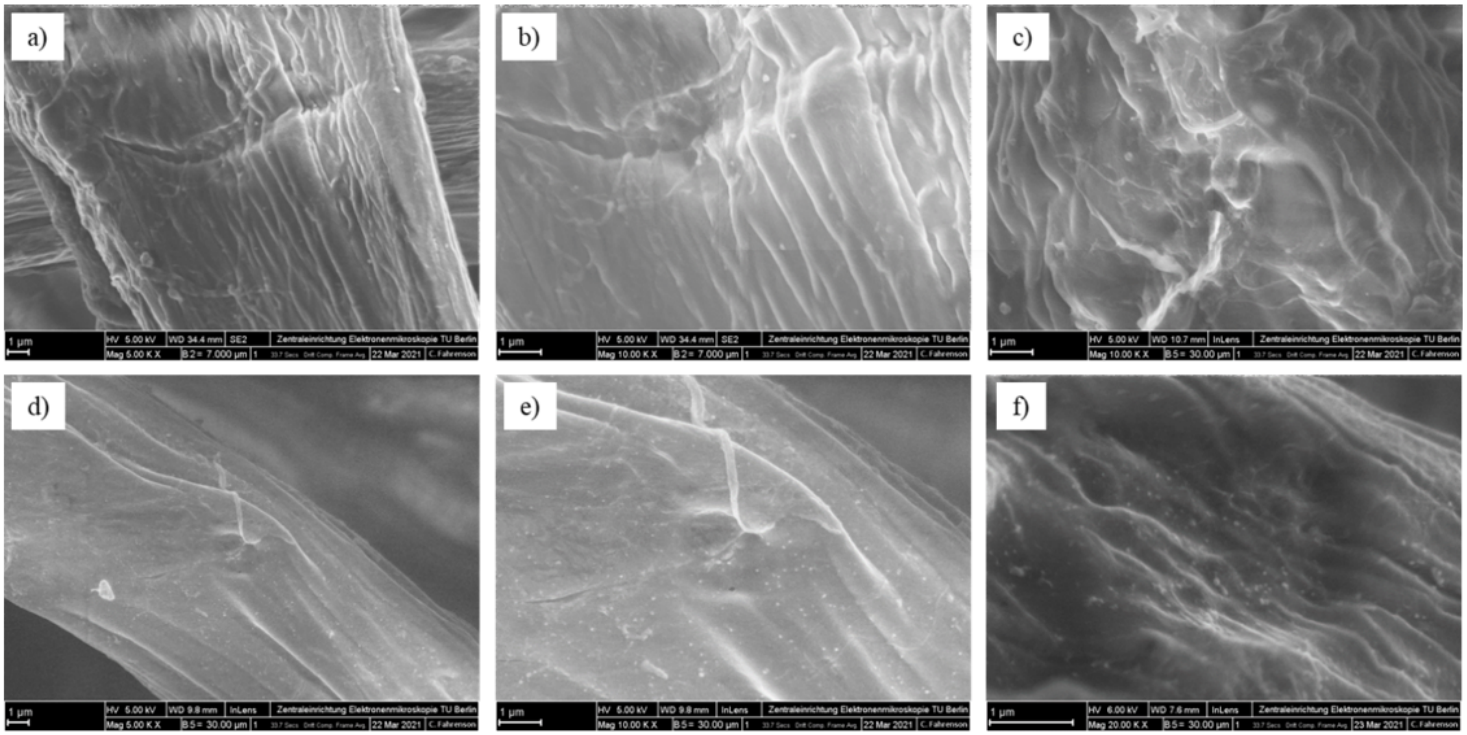

Figure 6

Field emission scanning electron microscopy (FESEM) study of Solucell.Pd.Gluc (a-c) and CMFE.Pd.Gluc (d-f).

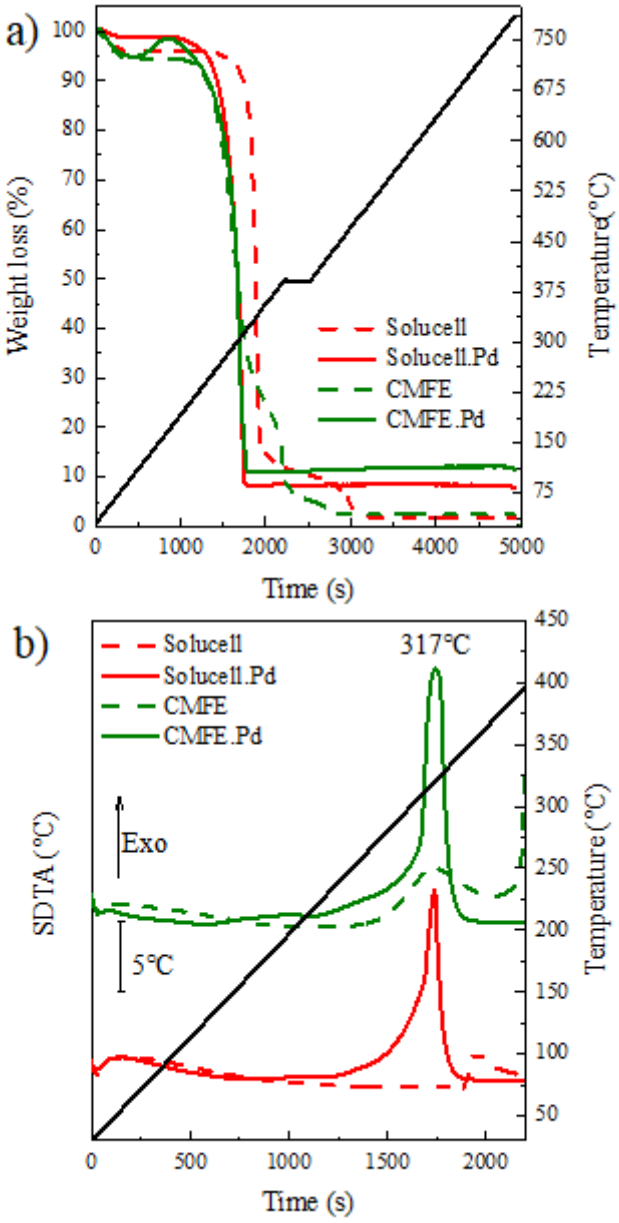

Figure 7

Thermogravimetric studies of the fibers: a) TGA and b) SDTA.

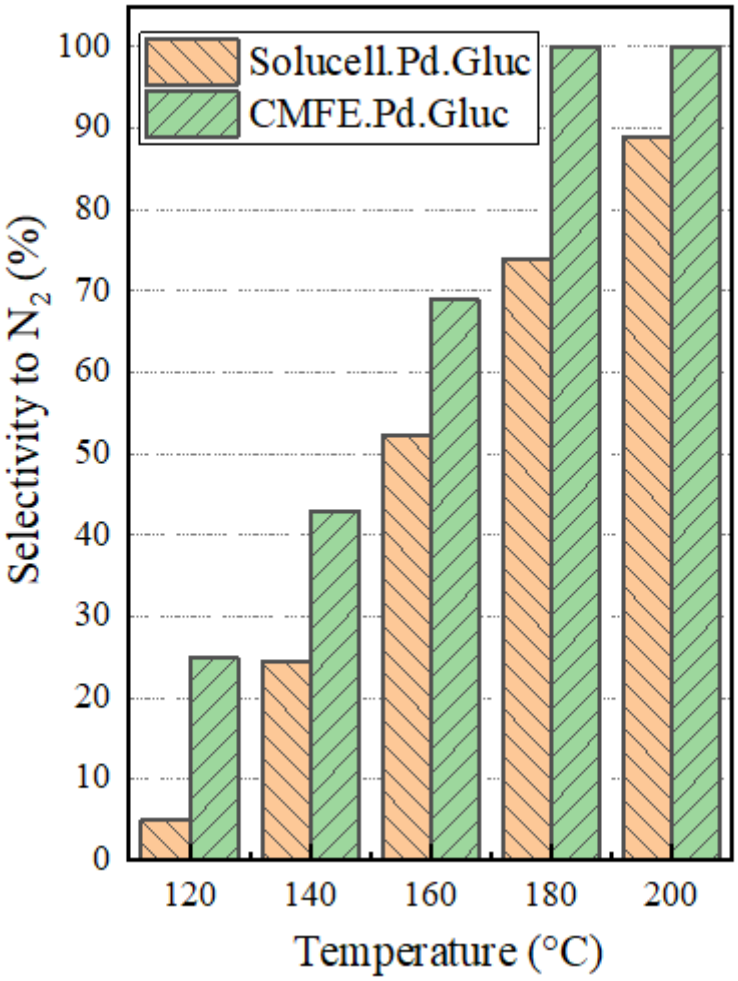

Figure 8

Catalytic performance of the prepared fibers. NO conversion was complete in the studied range of temperature. Selectivity to N2, SN2 = [NO]0 - 2[N2O] / [NO]0.

Supplementary Files

This is a list of supplementary files associated with this preprint. Click to download.

- SUPLEMENTARYINFORMATIONGIORIAGUTIERREZRevision2304.docx
- GraphicalAbstract.png
- Highlights.docx
- Schema1.png